Analysis of gene mutation in plant cell wall by dielectric relaxation

Frédéric Roig, Eric Dantras, Jacqueline Grima Pettenati, Colette Lacabanne

doi:10.1088/0022-3727/45/29/295402

Analysis of gene mutation in plant cell wall by dielectric relaxation

Frédéric Roig[1], **Eric Dantras**[1], **Jacqueline Grima-Pettenatti**[2] **and Colette Lacabanne**[1]

[1] Physique des Polymères, Institut Carnot CIRIMAT, Université Paul Sabatier, 118 route de Narbonne, 31062 Toulouse Cedex, France
[2] Génomique fonctionnelle de l'Eucalyptus, Laboratoire de Recherche en Sciences Végétales UMR CNRS 5546, Université de Toulouse, 24 chemin de Borde-Rouge, BP 42617 Auzeville, 31326 Castanet Tolosan, France

E-mail: dantras@cict.fr

Abstract

Arabidopsis Thaliana is a plant composed mainly of cellulose and lignin. Geneticists need techniques able to make differences at the molecular level between modified plants (DML6, CAD C/D) and non-modified ones. Thermo-stimulated current (TSC) analysis is a promising route to identify gene mutations. For the non-modified plant, at low temperatures, TSC thermograms highlight three dielectric relaxation modes. From −150 to −110 °C, $\gamma_{\text{Cellulose}}$ is attributed to CH_2OH and –OH groups of cellulose. Between −110 and −80 °C, β_{Lignin} is detected. From −80 to −40 °C, $\beta_{\text{Cellulose}}$ is characteristic of the molecular mobility of glycosidic linkages. For the CAD C/D modified plants, only $\gamma_{\text{Cellulose}}$ and β_{Lignin} are observed; due to analogous enthalpy values, those modes have the same molecular origin as in the non-modified plant. So, the β_{Lignin} mode is associated with the molecular mobility of the lignin-OH groups. The CAD C/D gene mutation changes the chemical structure of lignin, which promotes hydrogen bonds in the network and inhibits molecular mobility of glucosidic rings. It is also interesting to note that the DML6 gene mutation induces a higher cooperativity of this $\beta_{\text{Cellulose}}$ relaxation than in wild vegetal composites. In fact, this mutation promotes molecular mobility of glycosidic rings thanks to $\beta_{1\text{–}4}$ glycosidic linkages.

1. Introduction

Arabidopsis Thaliana is a member of the Cruciferae family with a broad natural distribution throughout North America, Europe and Asia [1]. It was chosen in the 1980s by biologists as a model plant. Key events in the development and use of Arabidopsis as a model plant go back in time to 1907. Friedrich Laibach initiated the use of this plant for experimental biology. In 1943, he highlighted the suitability of Arabidopsis as a model for genetic and biological research because this plant produced several descendants; it developed rapidly and was easy to cultivate in a small space. Moreover, it had a relatively low chromosome number [2]. In 1947, Erna Reinholtz showed the possibility of inducing mutations in Arabidopsis using x-ray irradiation [3]. The *Arabidopsis* community became organized in 1964 when *Arabidopsis* Information service (AIS) began its publication. One year later, the first *Arabidopsis* conference was held at Göttingen in Germany. The discovery in 1977 that *Agrobacterium Tumefaciens* could transfer its DNA to the nuclear genome of higher plants indicated that gene transfer to plant was possible [4]. The adoption of *Arabidopsis* as a model plant, followed by the current revolution in plant genetics occurred in the early 1980s. Key factors which helped biologists to choose *Arabidopsis* were its advantages in comparison with other species. Thanks to its small genome, informative mutations could be analysed easily [5] and it was convenient for gene cloning. Then, biologists chose *Arabidopsis* as a model plant; they focused on this plant and much progress has been made in this direction by scientists recently. Genome of *Arabidopsis* was the first genome of a plant which was sequenced [6].

In all plant materials, the major polymers constituting the cell walls are cellulose, lignin and hemicelluloses. In order to optimize the resource of the biomass plant, geneticists studied the cell wall composition [7]. Cellulose and hemicelluloses are polysaccharides well known to scientists in contrast to lignin. Lignin is a plant-specific phenolic polymer. The interest in lignification resulted from the identification of

this process as important in plant biology. Lignification is essential to render vessels waterproof and impart strength to fibres. Moreover, lignin is a physical barrier against pathogens. Hence, geneticists try to understand lignification. This biological process results from the polymerization of three types of monolignols: p-Coumaryl alcohol, Coniferyl alcohol and Sinapyl alcohol. After polymerization, these alcohols form p-Hydroxyphenyl units (H), Guaiacyl units (G) and Syringyl units (S). H unit is a phenolic cycle. G unit is also a phenolic cycle, which earns a methoxyl group at position three and S unit earns two methoxyl groups at positions three and five [8]. The formed polymer is reticulated. Moreover, better knowledge of lignification would improve chemical pulping, natural ruminant digestibility and biomass conversion to ethanol [9–11]. Consequently, geneticists are interested in Arabidopsis mutants of the monolignol biosynthesis pathway with impact on lignification [12–17].

Thermo-stimulated current (TSC) analysis is well suited to study molecular mobility of vegetal polymers. In a previous work on cellulose, we demonstrated the high resolution power of this technique [18]. At low temperatures, cellulose has two dielectric relaxation modes: the γ mode associated with side group reorientation of glycosidic rings and the β mode assigned to localized movements of the $\beta_{1\text{–}4}$ glycosidic bonds of cellulose. We analysed the evolution of these modes with increasing moisture content and we observed, accordingly with Montès *et al* [19–21], that the β relaxation mode was not always detectable by dynamic dielectric spectroscopy. Contrarily, by TSC, the latter mode can be followed for each state of hydration. Moreover, a study of poplar cell wall by dielectric techniques shows the contribution of cellulose and lignin in the chain dynamics of vegetal composites [22]. Consequently, molecular mobility can become a tool for identifying mutation and lignin structure elucidation. TSC is a promising route to identify gene mutation in *Arabidopsis Thaliana*. Here, we present TSC data from *Arabidopsis Thaliana* and mutants in two pathway enzymes COMT and CAD C/D. Downregulating these enzymes affects the structure and composition of lignin.

2. Experimental section

2.1. Materials

The cellulose and lignin specimens were provided by Sigma-Aldrich. Cellulose is a white microcrystalline powder (20 μm) extracted from cotton linters, with a number-average molecular weight between 36 000 and 40 000. The degree of polymerization is between 222 and 246. Lignin is a brown powder extracted from sugar cane. Samples of *Arabidopsis Thaliana* are of three types: a wild plant and two modified plants also called mutants. The first mutation, called DML6, affects the COMT gene, which downregulates caffeate/5-hydroxyferulate O-methyltransferase (COMT), an enzyme involved in the methylation of the precursors of sinapyl alcohol (a monomer of lignin). It leads systematically, in all examined species, to a striking decrease in syringyl (S) units and the production of unusual 5-hydroxyguaiacyl units (5-OH-G) [7, 8, 15, 23]. The second mutation, called CAD C/D, is a double mutation C and D on CAD gene, which affects the last step of lignin's monomer synthesis in decreasing the proportion of S units and guaiacyl (G) units in favour of sinapaldehyde and coniferaldehyde synthesis [8, 15, 17, 24]. Each stem of the plant was ground by a Dangoumeau ball mill to obtain powder. All powder samples (cellulose, lignin and different plants) were pressed under a controlled pressure of 75 MPa to form pellets.

2.2. Method: thermo-stimulated current

TSC measurements were carried out with home-made equipment previously described [25]. Pellets ($\phi = 0.8$ cm) were inserted between two steel plate electrodes. The sample cell was filled with dry helium. For recording complex thermograms, the sample was polarized by an electrostatic field $E_p = 780\,\mathrm{kV\,m^{-1}}$ for $t_p = 2$ min over a temperature range from the polarization temperature T_p down to the freezing temperature T_0. Then, the field was turned off and the depolarization current was recorded with a constant heating rate ($q_h = +7\,^\circ$C/min); the equivalent frequency of the TSC spectrum was $f_{eq} \sim 10^{-2}$–10^{-3} Hz. Elementary TSC thermograms were obtained with a poling window of 5 °C. Then, the field was removed and the sample cooled down to a temperature $T_{cc} = T_p - 40\,^\circ$C. The depolarization current was normalized to be homogeneous with dipolar conductivity σ and it was recorded with a constant heating rate q_h. A series of elementary thermograms was recorded by shifting the poling window by 5 °C towards higher temperatures.

In this procedure each elementary thermogram can be considered as a Debye process characterized by a single relaxation time $\tau(T)$. The temperature dependence of the relaxation time can be determined by the following equation:

$$\tau(T) = \frac{1}{q \times I(T)} \cdot \int_T^{T_f} I(T) \cdot \mathrm{d}T, \tag{1}$$

where q is the heating rate and $I(T)$ is the temperature-dependent depolarization current that vanishes at T_f.

In the materials studied in this work, the variation of the relaxation times $\tau(T)$ of all elementary spectra versus $1/T$ is linear and it obeys the Arrhenius–Eyring equation:

$$\tau(T) = \frac{h}{k_B T} \exp\left[-\frac{\Delta S}{R}\right] \exp\left(\frac{\Delta H}{RT}\right) = \tau_0 \exp\left[\frac{\Delta H}{RT}\right], \tag{2}$$

where R is the ideal gas constant, k_B is the Boltzmann constant, h is the Planck constant, ΔH is the activation enthalpy, ΔS is the activation entropy and τ_0 the pre-exponential factor.

According to the analysis of Starkweather [26–28], activation enthalpy is the sum of two contributions: theoretical enthalpy related to $\Delta S = 0$ and entropic enthalpy $\Delta S \neq 0$. Then

$$\Delta H = \Delta H^{\neq}(\Delta S = 0) + T\,\Delta S^{\neq}. \tag{3}$$

For relaxations having no activation entropy, equation (3) is reduced to the following relationship:

$$\Delta H = \Delta H^{\neq} = RT\left[1 + \ln\left(\frac{k_B \cdot T}{2\pi h \cdot f_{eq}}\right)\right], \tag{4}$$

where $f_{eq} \cong 10^{-3}$ Hz is the equivalent frequency of TSC.

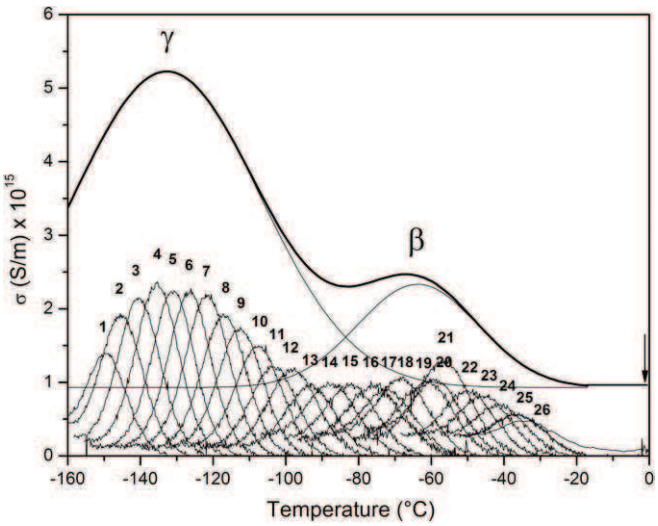

Figure 1. Complex TSC thermogram with the corresponding elementary thermograms for the γ and β relaxation modes of cellulose from -160 to 0 °C at 7 °C min^{-1}.

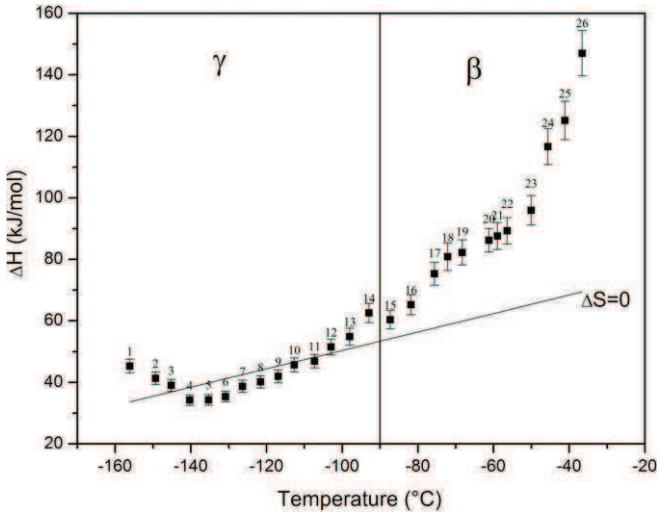

Figure 2. Activation enthalpy versus temperature for the elementary thermograms constituting the low-temperature relaxation modes of cellulose.

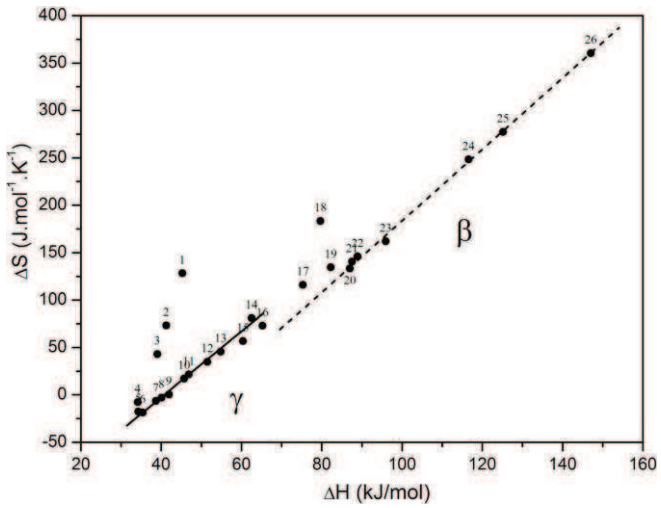

Figure 3. Compensation diagram of γ and β secondary relaxation modes of cellulose.

According to the Hoffman, Williams and Passaglia [29] model, activation entropy ΔS_n and activation enthalpy ΔH_n are linked to the size of the mobile entity. A linear relation exists between entropy and enthalpy which defines a compensation phenomenon [29–33]:

$$\Delta S_n = \frac{\Delta H_n}{T_C} - R \ln\left(\frac{\tau_C k_B \cdot T}{h}\right), \qquad (5)$$

where T_C is the compensation temperature and τ_C is the compensation time.

3. Results and discussion

3.1. Cellulose

Cellulose was studied in the low-temperature range by TSC. The normalized depolarization current σ is plotted versus temperature in figure 1. From -160 to 0 °C, we observe a complex thermogram which highlights two relaxation modes: γ and β. The γ relaxation mode is characterized by an intense and broad peak with a maximum at -135 °C. The β relaxation mode is defined by a shoulder with a maximum at -65 °C. Thermogram profiles are adjusted by Gaussian functions to differentiate each relaxation mode. These two relaxations modes are resolved experimentally into a series of elementary thermograms described well by a discrete distribution of relaxation times. Elementary thermograms with higher intensity correspond to the maximum of the relaxation mode.

The analysis of the series of elementary thermograms permits us to obtain the activation parameters. Figure 2 represents the evolution of the activation enthalpy ΔH versus temperature. Two different behaviours are underlined. From -160 to -90 °C, the enthalpy values follow Starkweather's line which is characteristic of localized mobility. Contrarily, from -90 to -20 °C, the enthalpy values move away progressively from Starkweather's line, which is indicative of a delocalized mechanism. The compensation diagram reported in figure 3 confirms the existence of two different behaviours defined by two compensation phenomena. From -160 to -90 °C, the γ relaxation mode of cellulose with enthalpy values from 30 to 60 kJ mol^{-1} is due to a localized cooperative molecular mobility, whereas from -90 to -20 °C, the β relaxation mode of cellulose with enthalpy values from 60 to 150 kJ mol^{-1} is due to a delocalized cooperative molecular mobility.

According to the literature, the γ relaxation mode of cellulose is attributed to the molecular mobility of lateral groups of glycosidic rings (–OH and –CH_2OH) [18, 34–44] and the β relaxation mode of cellulose is associated with the molecular mobility of glycosidic rings thanks to β_{1-4} glycosidic bonds | [18, 36–44].

3.2. Lignin

Lignin was studied by TSC in the low-temperature range. The normalized depolarization current σ is plotted versus

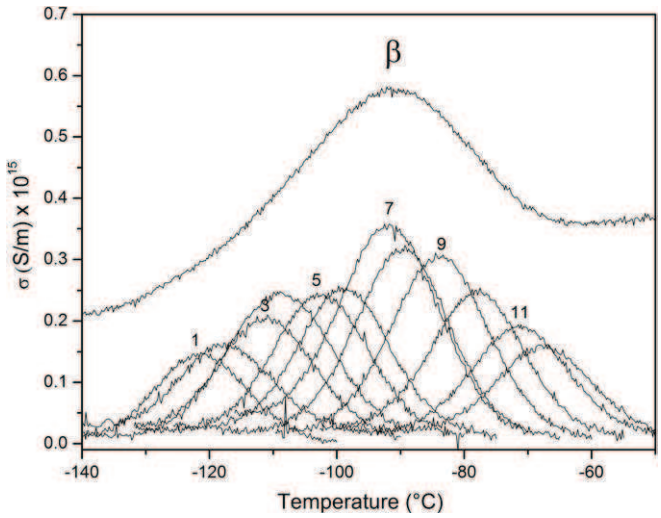

Figure 4. Complex TSC thermogram with their associated elementary thermograms for β relaxation mode of lignin from -140 to -50°C at 7 °C min^{-1}.

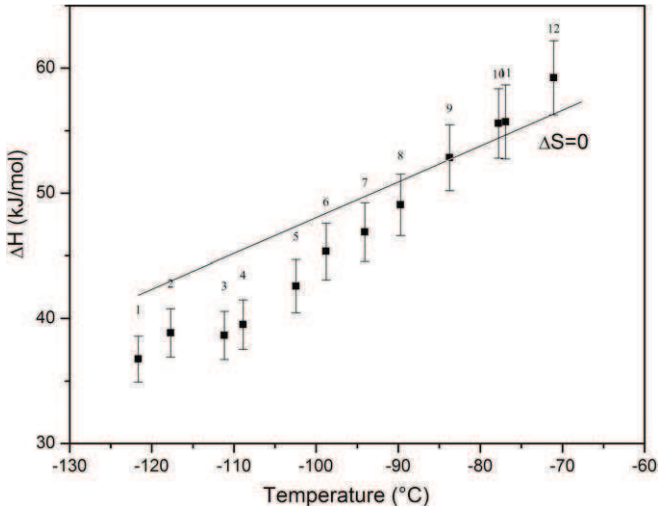

Figure 5. Activation enthalpy versus temperature for the elementary thermograms constituting the low-temperature relaxation mode in lignin. Solid line is Starkweather's line and theoretical enthalpy is represented ($\Delta H^{\neq}(\Delta S = 0)$).

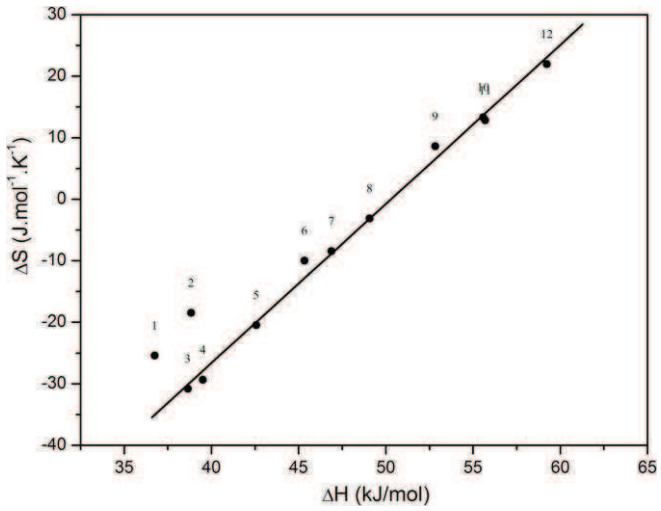

Figure 6. Compensation diagram of β relaxation mode of lignin (solid line shows the linear behaviour).

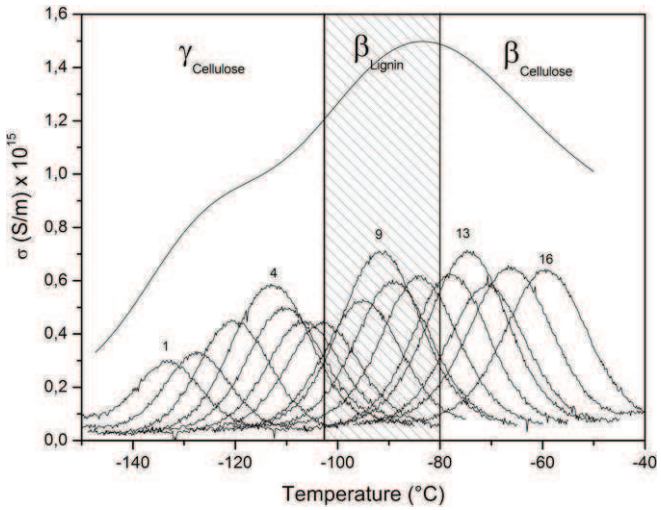

Figure 7. Complex TSC thermogram from -150 to -40°C (solid line for the higher values of σ (Sm^{-1})) and the corresponding elementary thermograms for low-temperature relaxation modes of *Arabidopsis Thaliana* at 7 °C min^{-1}.

temperature in figure 4. The complex thermogram observed from -140 to -50 °C highlights a β relaxation mode characterized by a broad peak with a maximum at -90 °C, which is resolved into elementary thermograms. Their analysis permits us to plot, in figure 5, the activation enthalpy ΔH versus temperature: the enthalpy values, ranged between 35 and 60 kJ mol^{-1}, are close to Starkweather's line, characteristic of localized molecular mobility. Figure 6 shows the variation of activation entropy ΔS versus enthalpy activation ΔH and it reveals a compensation phenomenon. Hence, the molecular origin of this relaxation mode may be linked with the polar groups of lignin. However, contrary to other polymers, which constitute the cell wall, chemical composition of lignin cannot be determined exactly [11, 45, 46]. The origin of this complexity is due to polymerization conditions of lignin and natural diversity. The different factors influencing polymerization and lignin synthesis are recapitulated by Terashima [47].

3.3. *Arabidopsis Thaliana* plant

Arabidopsis Thaliana was also studied in the low-temperature range by TSC. The normalized depolarization current σ versus temperature is plotted in figure 7. The complex thermogram plotted from -150 to -40 °C highlights a shoulder around -120 °C and a broad peak with a maximum at -85 °C. The elementary thermograms allow us to distinguish three relaxation modes. Thanks to the comparison with extracted cell wall polymers—cellulose (figure 1) and lignin (figure 4), we can attribute each relaxation mode of the vegetal composite to a cell wall polymer. In order of increasing temperature, we have $\gamma_{\text{Cellulose}}$, β_{Lignin} and $\beta_{\text{Cellulose}}$. The enthalpy thermogram of these relaxations is reported in figure 8. Three series of points are highlighted. All enthalpy values are close to

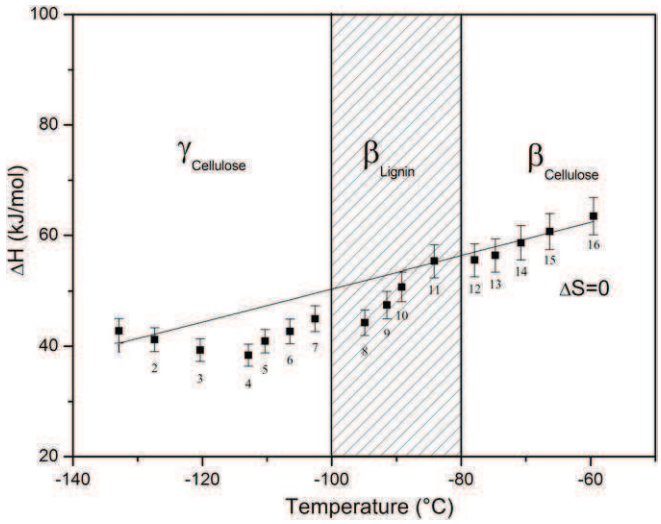

Figure 8. Activation enthalpy versus temperature for the elementary thermograms constituting the low-temperature relaxation modes in *Arabidopsis Thaliana*. Solid line is Starkweather's line and theoretical enthalpy is represented ($\Delta H^{\neq}(\Delta S = 0)$).

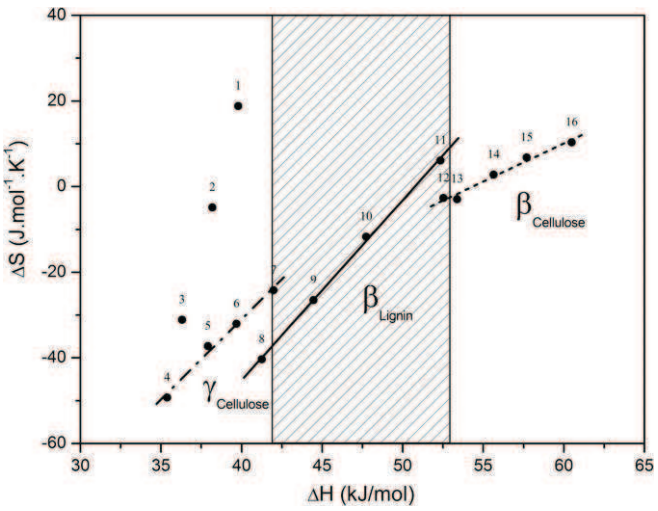

Figure 9. Compensation diagram of the low-temperature relaxation modes of *Arabidopsis Thaliana*.

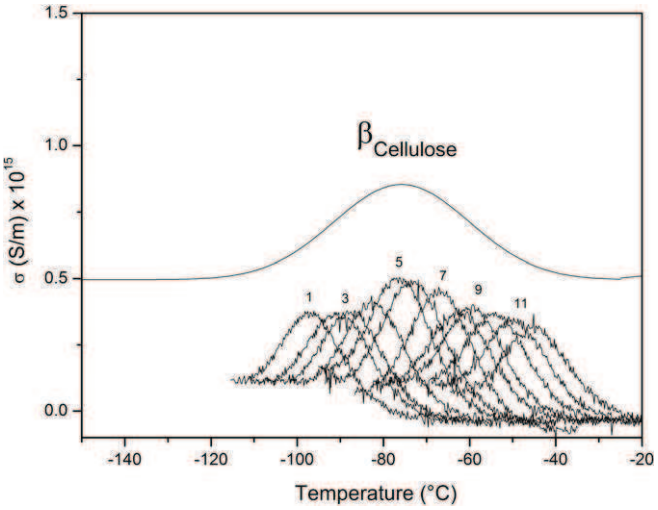

Figure 10. Complex TSC thermogram from −150°C to −20°C and the corresponding elementary thermograms for $\beta_{\text{Cellulose}}$ relaxation mode of mutant plant called DML6 at 7 °C min^{-1}.

Starweather's line: all these relaxations are localized. For $\gamma_{\text{Cellulose}}$ and β_{Lignin}, the mobility is also localized in the extracted polymers. Contrarily, for $\beta_{\text{Cellulose}}$, the molecular mobility is localized in the vegetal composite and delocalized in extracted cellulose. This difference may be explained by specific intra- and intermolecular interactions between cell wall polymers in the composite. We will comment on this phenomenon later on, in the next section. The compensation diagram (figure 9) shows that the three relaxation modes observed previously follow, respectively, a compensation law. At low temperatures *Arabidopsis Thaliana* has three cooperative relaxations modes. From −150 °C to −100 °C, with enthalpy values ranging between 35 and 45 kJ mol^{-1}, $\gamma_{\text{Cellulose}}$ relaxation mode is due to the localized cooperative mobility of lateral groups of glycosidics rings of cellulose (–OH and –CH_2OH) [18, 35, 42, 44]. In the temperature range −100 to −80 °C, with enthalpy values varying from 40 to 55 kJ mol^{-1}, β_{Lignin} relaxation mode is associated with localized cooperative molecular mobility. The origin of this relaxation will be expanded in the next section with the study of mutants. $\beta_{\text{Cellulose}}$ is characterized in the vegetal composite by a compensation phenomenon characteristic of a cooperative behaviour in the temperature range from −80 to −40 °C with enthalpy values between 55 and 60 kJ mol^{-1}. The origin of this relaxation mode is the molecular mobility of glycosidic rings thanks to $\beta_{1\text{–}4}$ glycosidic bonds [18, 42, 44].

3.4. Mutants of Arabidopsis Thaliana

3.4.1. DML6 mutant. In the low-temperature range, the normalized depolarization current σ versus temperature of Arabidopsis mutant, called DML6, is plotted in figure 10, which shows a relaxation mode between −120 and −20 °C with a maximum at −75 °C. Due to its temperature location, we can attribute this relaxation mode to the β relaxation mode of cellulose. The experimental resolution into elementary thermograms permits us to estimate the activation parameters and to confirm this hypothesis. Figure 11 represents the evolution of activation enthalpy versus temperature. The enthalpy values move away from Starkweather's line. So this relaxation mode is delocalized like the β relaxation mode of extracted cellulose (figure 2). Moreover, this relaxation mode, which corresponds to enthalpy values ranging between 55 and 105 kJ mol^{-1}, is characterized by a compensation phenomenon (figure 12). The relaxation mode of mutant DML6 is defined by a compensation phenomenon and a cooperative behaviour. It is attributed to $\beta_{\text{Cellulose}}$. The compensation diagram in figure 12 compares *Arabidopsis Thaliana* with its DML6 mutant. We can see that the mutant plant does not have $\gamma_{\text{Cellulose}}$ and β_{Lignin} relaxation modes. This gene mutation inhibits molecular mobility associated with lignin and molecular mobility of lateral groups of cellulose. Concerning $\beta_{\text{Cellulose}}$, the DML6 gene mutation induces a higher cooperativity of this relaxation than in the wild vegetal composite. In fact, this mutation promotes molecular mobility of glycosidic rings thanks to $\beta_{1\text{–}4}$ glycosidic linkages.

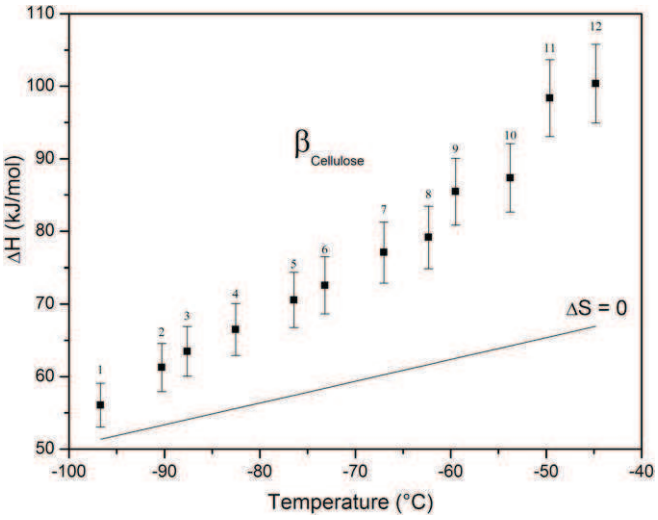

Figure 11. Activation enthalpy versus temperature for the elementary thermograms constituting the $\beta_{\text{Cellulose}}$ relaxation mode in DML6 mutant.

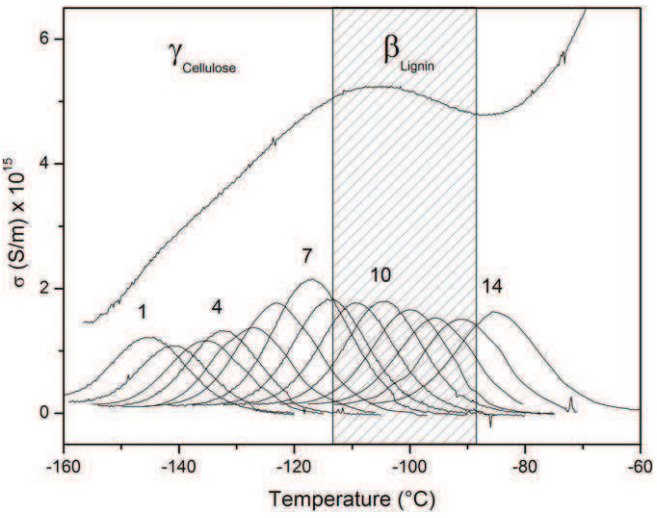

Figure 13. Complex TSC thermogram and the corresponding elementary thermograms for low-temperature relaxation modes of mutant plant called CAD C/D at 7 °C min^{-1} from −160 to −40°C.

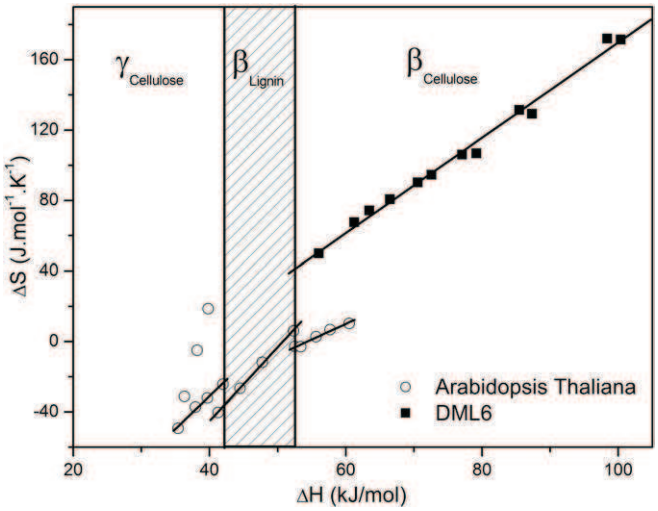

Figure 12. Comparison of compensation diagrams of modified plant (DML6) and *Arabidopsis Thaliana*.

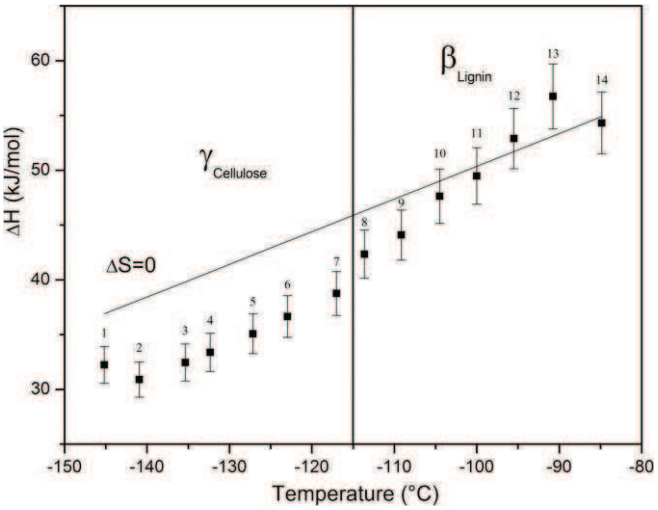

Figure 14. Activation enthalpy versus temperature for the elementary thermograms constituting the low-temperature relaxation modes in CAD C/D mutant. Solid line is Starkweather's line and theoretical enthalpy is represented ($\Delta H^{\neq}(\Delta S = 0)$).

3.4.2. CAD C/D mutant. Figure 13 represents the depolarization current σ versus temperature of the Arabidopsis mutant called CAD C/D. In the low-temperature range, this mutant presents two relaxations modes. These relaxations are identified thanks to experimental resolution. We observe two elementary thermograms more intense than the others at −105 and −115 °C. Due to the temperature location, we may, respectively, attribute these relaxations to $\gamma_{\text{Cellulose}}$ and β_{Lignin}. In figure 14, all the points are close to Starkweather's line ($\Delta S = 0$) so the different relaxation modes are localized. Moreover, due to analogous enthalpy values between $\gamma_{\text{Cellulose}}$ and β_{Lignin} of the modified plant, $\gamma_{\text{Cellulose}}$ is attributed to the molecular mobility of hydroxyl groups of cellulose, and β_{Lignin} is associated with the molecular mobility of hydroxyl groups of lignin. In the mutant CAD C/D the proportion of hydroxyl groups is more important than in the non-modified plant [23, 24]. Hence, the molecular mobility of OH entities masks the molecular mobility of glycosidic linkages. This explains why the $\beta_{\text{Cellulose}}$ mode is not observed in the modified plant (figure 2). The compensation diagram in figure 15 reveals that the CAD C/D mutant admits two compensation phenomena, associated with $\gamma_{\text{Cellulose}}$ and β_{Lignin} instead of three ($\gamma_{\text{Cellulose}}$, β_{Lignin} and $\beta_{\text{Cellulose}}$) for the non-modified plant. These three relaxation modes are observed with a specific enthalpy range. $\gamma_{\text{Cellulose}}$ is measured between 30 and 42 kJ mol^{-1}, β_{Lignin} is highlighted between 42 and 55 kJ mol^{-1} and for enthalpy values above 53 kJ mol^{-1} we can observe $\beta_{\text{Cellulose}}$. This type of diagram allows us to identify the cooperative relaxation modes.

4. Conclusion

TSC is well suited to identify the influence of gene mutation on the physical structure of a natural plant. The evolution of molecular mobility is clearly exhibited. Thanks to TSC, we distinguish, on a molecular scale, native *Arabidopsis Thaliana*

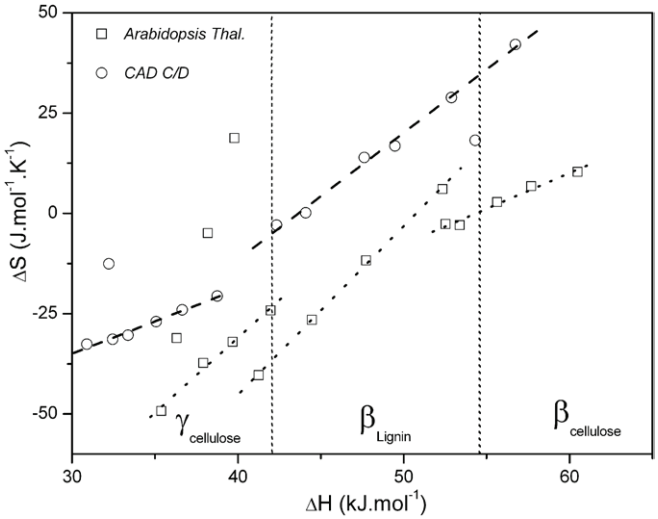

Figure 15. Comparison of compensation diagrams of CAD C/D mutant and *Arabidopsis Thaliana*.

and its mutants. In fact, the localized molecular mobility is characteristic of the different vegetal composites. Moreover, each relaxation is identified by comparison with the localized molecular mobility of extracted polymers. The integrity of the extracted polymer cell wall is maintained in the native *Arabidopsis Thaliana* plant. According to a previous work, $\gamma_{\text{Cellulose}}$ relaxation mode is attributed to the molecular mobility of the side groups of glycosidic rings. The origin of $\beta_{\text{Cellulose}}$ relaxation mode is localized movements of glycosidic rings thanks to $\beta_{1\text{–}4}$ glycosidic bonds. The molecular origin of β_{Lignin} remains unclear. Thanks to CAD C/D mutant, β_{Lignin} mode is associated with the molecular mobility of lignin polar groups (-OH). In this mutant, the genetic modification changes the chemical structure of lignin and increases the proportion of hydroxyl groups. The increase in hydroxyl group ratio promotes hydrogen bonds which inhibit molecular mobility of glucosidic rings. This behaviour contrasts with the one of mutant DML6, which promotes the molecular mobility of glycosidic rings thanks to $\beta_{1\text{–}4}$ glycosidic bonds and decreases the hydrogen bond network influence.

References

[1] Meinke D W, Cherry J M, Dean C, Rounsley S D and Koornneef M 1998 *Science* **282** 662, 679–682
[2] Somerville C and Koornneef M 2002 *Nature Rev. Genetics* 883–9
[3] Meyerowitz E M 2001 *Plant Physiol.* **125** 15–19
[4] Chilton M D, Drummond M H, Merlo D J, Sciaky D, Montoya A L, Gordon M P and Nester E W 1977 *Cell* **11** 263–71
[5] Somerville C R and Ogren W L 1979 *Nature* **280** 833–6
[6] The Arabidopsis Initiative 2000 *Nature* **408** 796–815
[7] Boudet A M, Kajita S, Grima-Pettenati J and Goffner D 2003 *Trends Plant Sci.* **8** 576–81
[8] Jouanin L and Lapierre C 2006 *Cahiers Agricultures* **15** 179–85
[9] Stewart J J, Akiyama T, Chapple C, Ralph J and Mansfield S D 2009 *Plant Physiol.* **150** 621–35
[10] Bjurhager I, Olsson A M, Zhang B, Gerber L, Kumar M, Berglund L A, Burgert I, Sundberg B and Salmén L 2010 *Biomacromolecules* **11** 2359–65
[11] Ke J, Laskar D D and Chen S 2011 *Biomacromolecules* **12** 1610–20
[12] Chapple C C S, Vogt T, Ellis B E and Somerville C R 1992 *Plant Cell* **4** 1413–24
[13] Ruegger M and Chapple C 2001 *Genetics* **159** 1741–9
[14] Franke R, Humphreys J M, Hemm M R, Denault J W, Ruegger M O, Cusumano J C and Chapple C 2002 *Plant J.* **30** 33–45
[15] Goujon T *et al* 2003 *Plant Mol. Biol.* **51** 973–89
[16] Sibout R, Eudes A, Pollet B, Goujon T, Mila I, Granier F, Séguin A, Lapierre C and Jouanin L 2003 *Plant Physiol.* **132** 848–60
[17] Sibout R, Eudes A, Mouille G, Pollet B, Lapierre C, Jouanin L and Séguin A 2005 *Plant Cell* **17** 2059–76
[18] Roig F, Dantras E, Dandurand J and Lacabanne C 2011 *J. Phys. D: Appl. Phys.* **44** 045403
[19] Montès H, Mazeau K and Cavaillé J Y 1997 *Macromolecules* **30** 6977–84
[20] Montès H, Mazeau K and Cavaillé J Y 1998 *J. Non-Cryst. Solids* **235–237** 416–21
[21] Montès H and Cavaillé J Y 1999 *Polymer* **40** 2649–57
[22] Jafarpour G, Dantras E, Boudet A and Lacabanne C 2008 *J. Non-Cryst. Solids* **354** 3207–14
[23] Ralph J *et al* 2001 *Phytochemistry* **57** 993–1003
[24] Grima-Pettenati J and Goffner D 1999 *Plant Sci.* **145** 51–65
[25] Teyssedre G and Lacabanne C 1995 *J. Phys. D: Appl. Phys.* **28** 1478–87
[26] Starkweather H W Jr 1981 *Macromolecules* **14** 1277–81
[27] Starkweather H W Jr and Avakian P 1989 *Macromolecules* **22** 4060–2
[28] Starkweather H W Jr 1990 *Macromolecules* **23** 328–32
[29] Hoffman J D, Williams G and Passaglia E 1966 *J. Polym. Sci.* C **14** 173–235
[30] Meyer W and Neldel H 1937 *Zeitschr. F. Techn. Physik* **12** 588–93
[31] Yelon A, Movaghar B and Branz H M 1992 *Phys. Rev.* B **46** 12244–50
[32] Crine J P 1984 *J. Macromol. Sci.* B **23** 201–19
[33] Crine J P 2005 *IEEE Trans. Dielectr. Electr. Insul.* **12** 1089–107
[34] Saad G R 1996 *Polym. Int.* **41** 293–9
[35] Saad G R 1997 *Polym. Int.* **42** 356–62
[36] Einfeldt J, Meißner D and Kwasniewski A 2000 *Macromol. Chem. Phys.* **201** 1969–75
[37] Einfeldt J, Meißner D, Kwasniewski A, Gruber E and Henricks R 2000 *Macromol. Mater. Eng.* **283** 7–14
[38] Meißner D, Einfeldt J and Kwasniewski A 2000 *J. Non-Cryst. Solids* **275** 199–209
[39] Einfeldt J, Meißner D and Kwasniewski A 2001 *Prog. Polym. Sci.* **26** 1419–72
[40] Einfeldt J and Kwasniewski A 2002 *Cellulose* **9** 225–38
[41] Einfeldt J, Meißner D and Kwasniewski A 2003 *J. Non-Cryst. Solids* **320** 40–55
[42] Einfeldt J, Meißner D and Kwasniewski A 2004 *Cellulose* **11** 137–50
[43] Jafarpour G, Dantras E, Boudet A and Lacabanne C 2007 *J. Non-Cryst. Solids* **353** 4108–15
[44] Jafarpour G, Roig F, Dantras E, Boudet A and Lacabanne C 2009 *J. Non-Cryst. Solids* **355** 1669–72
[45] Mohanty A K 2005 *Natural Fibers, Biopolymers and Biocomposites* (Boca Raton, FL: CRC Press)
[46] Saito K, Kato T, Takamori H, Kishimoto T and Fukushima K 2005 *Biomacromolecules* **6** 2688–96
[47] Terashima N 1990 *J. Pulp Paper Sci.* **16** 150–5